Biochimica et Biophysica Acta 1808 (2011) 1764–1771

Contents lists available at ScienceDirect

Biochimica et Biophysica Acta

journal homepage: www.elsevier.com/locate/bbamem

Microcin J25 membrane interaction: Selectivity toward gel phase

Fernando Dupuy, Roberto Morero *

Departamento Bioquímica de la Nutrición, INSIBIO-CONICET/UNT e Instituto de Química Biológica Dr. Bernabé Bloj, Universidad Nacional de Tucumán, Chacabuco 461 San Miguel de Tucumán, Tucumán T4000ILI, Argentina

ARTICLE INFO

Article history:
Received 23 December 2010
Received in revised form 14 February 2011
Accepted 22 February 2011
Available online 1 March 2011

Keywords:
Microcin
Membrane
Fluorescence quenching
Binding isotherm
Permeabilization

ABSTRACT

The interaction of the tryptophan-containing variant of microcin J25, MccJ25 I13W, with phosphatidylcholine membranes was studied by fluorescence spectroscopy techniques. The peptide was able to interact with dimiristoylphophatidylcholine and dipalmitoylphosphatidylcholine liposomes only when the membranes were in gel phase, as was demonstrated by the blue shift of the intrinsic fluorescence of MccJ25 I13W. The binding isotherm showed a cooperative partition of the peptide toward the membrane and the binding constant increased as the temperature decreased and the order parameter increased. No interaction with liquid crystalline membranes was observed. Studies of dynamic quenching of the fluorescence indicated that the peptide penetrated the lipid bilayer and was located primarily in the interfacial region. Our results suggest that MccJ25 I13W interacts with gel phase phospholipids and increases both its own affinity for the bilayer and the membrane permeability of small ions.

1. Introduction

Antimicrobial peptides are synthesized and secreted by organisms among plant, animal and prokaryotic kingdoms and have the ability to kill microorganisms. The mechanism of action of these peptides is highly variable, probably because of the few features in common they share with each other. The ability to permeabilize the plasma membrane of target cells precisely is a very general feature. In order to explain how peptides interact with and disrupt membranes, two types of models have been proposed [1–3]. The first model is termed the 'carpet' model, where at low concentrations, peptides lay across the surface of the membrane and, once a critical concentration is reached, disrupt bilayers in a detergent-like manner causing the formation of micelles and ultimately the disintegration of the membrane [4]. The second type is known as the barrel-stave model and involves the formation of discrete oligomeric pores that allow ions and other molecules to cross the membrane [3]. Variations of this are the 'toroidal pore' model, whereby the pore is composed of both peptide monomers and lipid head groups, and the aggregate model in which the peptides and lipids form informal aggregates within the membrane that permit ion leakage or peptide translocation across the membrane. In the beginning, membrane permeabilization was believed to be the sole event responsible for cell killing, although it was actually probed for only certain peptides. Moreover, it was shown that in some cases, depolarization of the plasma membrane alone did not ensure viability loss of sensible cells [5], suggesting that the killing effect mediated by antimicrobial peptides would involve multitarget strategies.

Microcins are a miscellaneous group of low-molecular weight peptides with antibiotic activity. They are produced by a number of *Enterobacteriaceae* species, mostly *Escherichia coli* strains [6,7]. Although most of the microcins inhibit enzymatic pathways, membrane interaction was also postulated to be part of their mechanism of action. Microcin J25 (MccJ25) is a 21-amino acid antimicrobial peptide that target certain human pathogens such as *Salmonella* and *Shigella* [8]. The sequence is rich in hydrophobic residues and the backbone is folded in an unusual lasso distinctive structure [9–11]: the γ-carboxyl of the side chain of Glu^8 and the N-terminal Gly^1 are covalently bonded and form an eight residue ring that is threaded by C-terminal tail (Fig. 1). This folding is maintained by steric hindrance between the aromatic side chains of Phe^{19} and Tyr^{20}, located on each side of the ring, and the residues of the ring [9–11]. MccJ25 exerts antimicrobial activity by means of a dual mechanism of action [12]: the peptide inhibits transcriptional activity by obstructing the RNA polymerase secondary channel [13–15] and affects, independently, the cytoplasmic membrane of *Escherichia coli* and *Salmonella enterica* serovars [12,16,17] . In this regard, it was shown that MccJ25 causes dissipation of the membrane electrical potential of *S. enterica* and inhibition of respiratory chain enzymes such as NADH, succinate and lactate dehydrogenase, decreasing oxygen consumption rates. The fact that MccJ25 is a membrane-active peptide was also supported by studies carried out on model systems, such as liposomes and Langmuir monolayers [18,19].

In this work, we performed a study of the interaction of a tryptophan-containing derivative of microcin J25, MccJ25 I13W, with model membranes by means of fluorescence spectroscopic methods. The results

* Corresponding author. Tel./fax: +54 381 4248921.
E-mail address: rdmorero@fbqf.unt.edu.ar (R. Morero).

0005-2736/$ – see front matter © 2011 Elsevier B.V. All rights reserved.
doi:10.1016/j.bbamem.2011.02.018

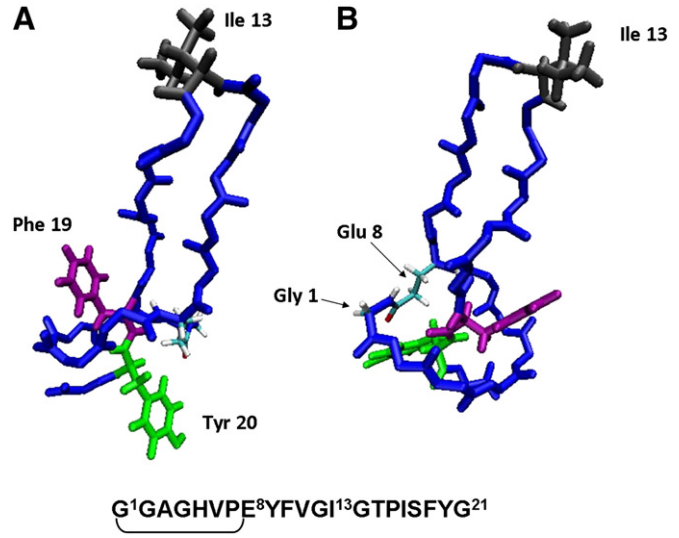

Fig. 1. Microcin J25 structure obtained from PDB file 1Q71. Lateral view (A) depicts the bulky side chains of residues Phe[19] and Tyr[20] and the residue Ile[13] which was replaced by tryptophan. Upper view (B) depicts the residue Ile[13] and the N-terminal ring, formed by amide bond between the sidechain of residue Glu[8] and the N-terminal Gly[1].

show unusually strong selectivity of peptide toward phospholipids bilayers in gel phase.

2. Materials and methods

2.1. Materials

1, 2-Dipalmitoyl-*sn*-glycero-3-phosphocholine (DPPC) and 1,2-dimyristoyl-*sn*-glycero-3 phosphocholine (DMPC) were obtained from Avanti Polar Lipids (Alabaster, AL). All chemicals used were of analytical grade. Potassium phosphate monobasic (KH_2PO_4), sodium phosphate dibasic (Na_2HPO_4), sodium chloride, Triton X-100, the spin labels 5-doxyl stearic acid (5DS) and 16-doxyl stearic acid (16DS) and N-acetyl-tryptophanamide (NATA) were purchased from Sigma-Aldrich (St. Louis, MO). 3,3′-Dipropylthiadicarbocyanine iodide ($DiSC_3$ (5)) was purchased from Molecular Probes–Invitrogen.

2.2. Mutagenesis and peptides purification

MccJ25 and MccJ25 I13W were purified from 2-l cultures of strain SBG231, harboring the corresponding plasmids as previously described [19]. The purity of the peptides was evaluated by analytical high performance chromatography in two different configurations of a Gilson HPLC system as follows: 20 µl of a 0.1 mg ml^{-1} solution of either MccJ25 or its variant, MccJ25 I13W, was loaded either on a µBondapak C18 column (10 µm, 3.9×300 mm Waters) and eluted in a linear gradient from 20 to 80% (v/v) methanol in trifluoroacetic acid (TFA) 0.1% (v/v), or on a X-Terra MS C8 column (5 µm, 4.6×250 mm, Waters) and eluted in a linear gradient from 0 to 60% (v/v) acetonitrile in 0.1% (v/v) TFA. Both MccJ25 and MccJ25 I13W peptides purified in our laboratory eluted as a single peak in these analytical chromatography systems.

2.3. Liposome preparation

DPPC (2 mM) and DMPC (2 mM) in chloroform were used as stock solutions for the preparation of dried films. The stock solutions were aliquoted to the bottom of clean glass and the solvent was evaporated under a gentle stream of N_2 gas. Trace of the solvent was removed under vacuum during 3 h. The dried lipid films were hydrated by adding the appropriate volume of buffer for a 1 mM phospholipid dispersion and by heating and vortexing the sample about 10 °C above the transition temperature of each lipid. The hydrated multillamelar suspension was then sonicated with a Branson tip sonicator for 30 min at temperatures higher than the transition temperature of the lipids. The small unilamellar vesicles were centrifuged at 8000×*g* for 10 min in order to eliminate titanium particles and multilamellar vesicles. Large unilamellar vesicles were prepared by extruding 10 times multilamellar vesicles through 100 nm polycarbonate filters (Whatman), in a stainless steel extruder operated under high pressure N_2 flow and heated above the main transition temperature of the phospholipids.

2.4. Fluorescence measurements

Fluorescence was recorded on an ISS-PC1 photon-counting spectrofluorimeter. Emission and excitation slits were 1 mm width (8 nm FWHH) and emission intensity background corrections were performed by subtracting the corresponding control without peptide using the Vinci software provided by the manufacturer. A computer-controlled stirrer device ensured constant mixing of the medium. The temperature inside the cuvette was measured with a thermocouple and adjusted to the desired value with a circulating water bath (Cole Parmer).

Peptide and phospholipid concentrations were always lower than 10 µM and 1 mM, respectively, in order to avoid inner filter effects ($\varepsilon_{278\ nm,\ MccJ25\ I13W} = 8714\ M^{-1}cm^{-1}$) and undesired light scattering in the different assays. Peptide solutions and vesicles suspensions were prepared in 10 mM KH_2PO_4, 100 mM Na_2HPO_4, 0.2 mM EDTA, pH 7.4 (phosphate buffer).

Fluorescence quenching assays were carried out at 27 °C by adding increasing amounts of cesium chloride from a 5 M stock solution to a mixture containing peptide and phospholipids vesicles in a 1:200 molar ratio. Peptide and quencher final concentration were 2.5 µM and 400 mM, respectively. The decrease of the fluorophore emission intensity produced by the increasing volume of the mixture during titration was negligible with respective to the cesium quenching effect.

From the fluorescence values obtained ($\lambda_{emission} = 353$ nm; $\lambda_{excitation} = 288$ nm) at different concentrations of cesium, Stern–Volmer graphs were constructed according to the following equation:

$$\frac{F_0}{F} = 1 + K_{SV}[Q]$$

where F_o and F are the peptide fluorescence intensities in the absence and in the presence of the quencher at concentration [Q], respectively. The Stern–Volmer constant (K_{SV}) was calculated from the slope of the curve and is proportional to the quencher accessibility to the peptide.

The depth of insertion of MccJ25 I13W into the lipid bilayer was studied by quenching of the peptide intrinsic fluorescence by the spin label probes 5-DS and 16-DS. The fluorescence emission at 335 nm, excited at 288 nm, was measured after addition of successive aliquots of methanolic stock solutions of the spin labels probes. The actual concentration of the probes inside the hydrophobic core of the phospholipids membranes $(Q)_l$ was calculated according to their corresponding partition coefficient ($K'_{pQ} = 12570$ and $K'_{pQ} = 3340$, for 5-DS and 16-DS, respectively) [20].

$$[Q]_l = \left(\frac{K'_{pQ}}{1 + K'_{pQ}\gamma[L]}\right).[Q]$$

2.5. Calculation of the partition coefficient of MccJ25 I13W

The peptide binding to the lipid bilayer was quantified by measuring the fluorescence increase at 335 nm as liposome aliquots were added. The increase in fluorescence intensity is proportional to the amount of peptide incorporated into the vesicles [21,22], so a binding

constant can be calculated by adjusting the experimental data to the following equation:

$$I = \frac{I_w + K_p^n \cdot \gamma_L [L]^n I_{max}}{1 + K_p^n \cdot \gamma_L [L]^n}$$

where I: fluorescence intensity at 335 nm; I_w: fluorescence intensity of peptide in buffer; K_p: partition coefficient; [L]: lipid concentration; I_{max}: fluorescence intensity of the peptide in lipid phase; n: cooperativity parameter; γ_L: molar volume (0.688 L mol^{-1} for DPPC).

2.6. Permeability assay

Large unilamellar vesicles were loaded with Li^+ by extrusion DPPC multilamellar vesicles in 100 mM Li_2SO_4, 10 mM HEPES, Li 0.2 mM EDTA, pH 7.4. Non-entrapped Li^+ ions were removed by gel chromatography (Sephadex G75) in a 1×10 cm column equilibrated and eluted with 100 mM Na_2SO_4 10 mM HEPES–Li 0.2 mM EDTA, pH 7.4. Differential permeability of the cations at both sides of the membrane can give rise a transmembrane potential, which can then be measured by means of the potential-sensitive probe $DiSC_3(5)$. The probe partition is enhanced and its fluorescence emission is self-quenched in the presence of transmembrane electrochemical gradients. The effect of MccJ25 I13W on the permeability of DPPC liposomes was studied by measuring the fluorescence emission of 0.5 μM $DiSC_3(5)$ added to a 1 mM phospholipid suspension, with excitation and emission wavelengths set at 622 and 677 nm, respectively.

3. Results

3.1. Peptide–membrane interaction

Studies on the interaction of liposomes with MccJ25 by intrinsic fluorescence spectroscopy were difficult to carry out because the primary structure of the peptide has two tyrosine and two phenylalanine residues but no tryptophan. As a consequence, the MccJ25 emission spectrum showed only features of Tyr residues, with a maximum at 303 nm and low sensitivity to environmental changes [23,24]. A slight decrease in the fluorescence intensity at low peptide: lipid ratio (1:100) was observed when the peptide was incubated with DPPC liposomes. On the other hand, the fluidity of DPPC liposomes was slightly altered by MccJ25 only at peptide/phospholipid ratios above 20. In order to study the interaction of the peptide with model membranes in a more sensitive system, we decided to obtain MccJ25 mutants in which some of peptide amino acids were replaced by tryptophan.

Replacement of isoleucine[13], which is located at the lasso region of the molecule (Fig. 1), by tryptophan led to the formation of an analogous, MccJ25 I13W, that could be purified by following the same protocol used for MccJ25 and preserved both antimicrobial activity (MIC = 40 nM against *S. enteritidis* serovar Newport) and physicochemical properties, like similar retention time in analytic HPLC and secondary structure, as assayed by infrared spectroscopy.

The variant peptide MccJ25 I13W showed a fluorescence emission maximum at 353 nm, indicating that the tryptophan residue is exposed to aqueous solvent (Fig. 2) and that no peptide aggregation occurred in the concentration range used in this work (0.5–10 μM).

By titrating a 2 μM aqueous solution of MccJ25 I13W with DPPC liposomes at 27 °C, two notable effects on the emission fluorescence spectrum of the peptide were observed: a marked blue shift of emission maximum, reaching a minimum value at 335 nm, and an increase in emission intensity (Fig. 2A). The effect was dependent on the amount of added lipid, reaching the maximum at 1:200 peptide:lipid molar ratio. However, the addition of DMPC liposomes to 2 μM MccJ25 I13W did not produce either of these two effects (Fig. 2B). Since these experiments were performed at 27 ° C, the physical state of the DMPC was liquid crystal phase ($T_{M\ DMPC}$ = 21 °C), whereas the physical state of DPPC corresponded to gel phase ($T_{M\ DPPC}$ = 41 ° C), suggesting a preferential interaction of MccJ25 I13W with gel phase membranes. However, in order to determine whether this effect could be also be related to the difference in the chain length of the phospholipids, fluorescence spectra of the peptide were measured in the presence of the same liposomes but at 12 °C, so that both membrane systems were under their T_M. As can be seen in Fig. 3, when the experiments were performed with DPPC and DMPC liposomes in the gel phase, the fluorescence spectra of MccJ25 I13W underwent similar changes, although the blue shift of the emission spectra and the increase in intensity were more pronounced for DPPC membranes (Fig. 3A) respective to DMPC liposomes (Fig. 3B) at the same peptide:phospholipid ratio. On the contrary, measurements carried out at 50 °C in (both kind of liposomes found in liquid crystal phase) no modifications of the fluorescence spectra were obtained (results not shown).

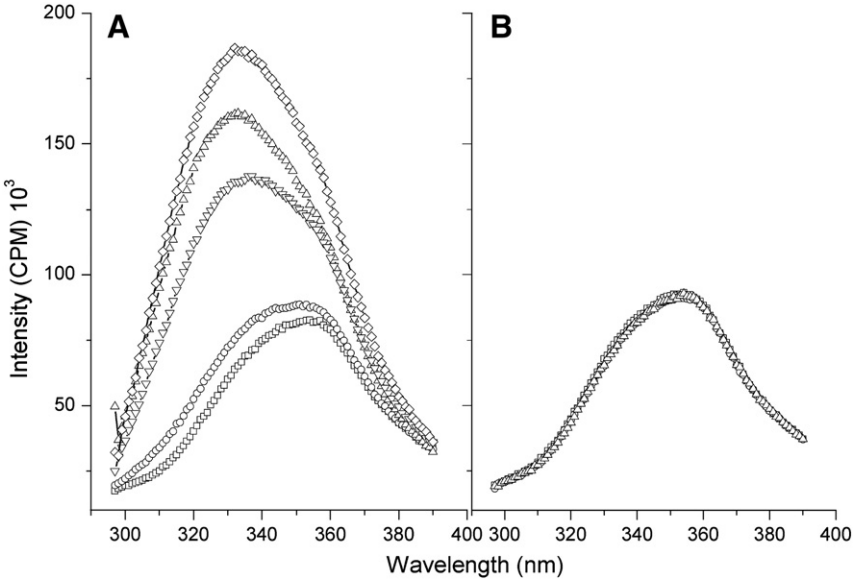

Fig. 2. Effect of addition of DPPC and DMPC liposomes on the fluorescence emission spectra of MccJ25I13W. MccJ25I13W (2.5 μM) dissolved in aqueous solution was incubated at 27 ° C and titrated different amounts of DPPC (A) or DMPC (B) liposomes. Emission spectra were recorded by excitation at 288 nm after incubating 5 min between successive vesicle addition. Peptide:lipid molar ratio were 1:0 (□), 1:20 (○), 1:100 (▽), 1:150 (△), and 1:200 (◊) for DPPC liposomes and 1:0 (□), 1:100 (○) and 1:200 (△) for DMPC liposomes.

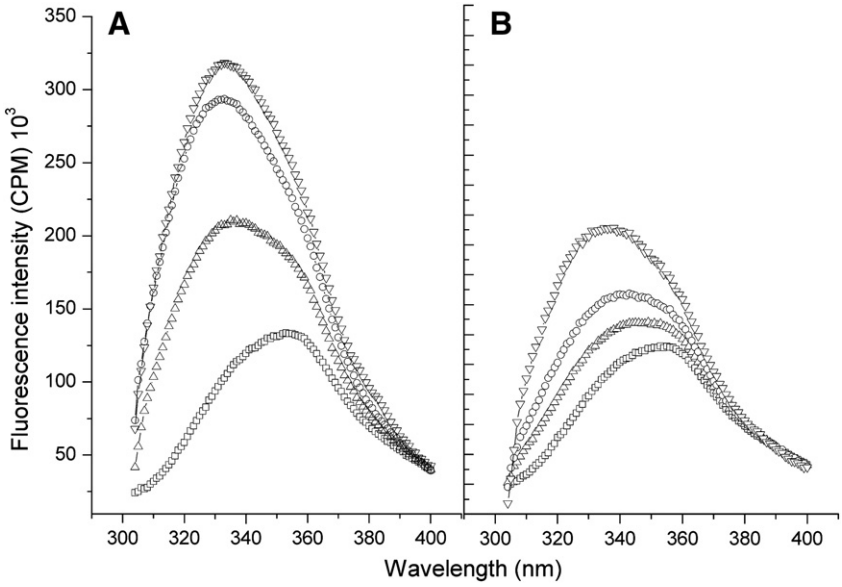

Fig. 3. Effect of DPPC and DMPC liposomes on the fluorescence emission spectra of MccJ25I13W. MccJ25I13W (2.5 μM) dissolved in aqueous solution was incubated at 12 °C and titrated with different amounts of DPPC (A) or DMPC (B) liposomes. Emission spectra were recorded by excitation at 288 nm. Peptide:lipid molar ratio were 1:0 (□), 1:50 (Δ), 1:100 (○) and 1:200 (▽).

3.2. Intrinsic fluorescence quenching of MccJ25 and MccJ25 I13W by water soluble quenchers

In order to determine whether the observed blue shift in emission spectra of MCCJ25 I13W in the presence of gel phase liposomes was due specifically to the partition of the peptide into the lipid bilayer, experiments were performed by measuring the accessibility of the Trp-containing peptide to the water soluble quencher Cesium chloride.

Addition of CsCl decreased the fluorescence emission of MccJ25 I13W in the absence of membranes, confirming that the Trp residue was exposed to the solvent at peptide concentrations of 2 μM (Fig. 4A), in accordance with the fluorescence emission maxima at 353 nm of the peptide dissolved in buffer. As a comparison, the quenching of NATA by CsCl yielded a higher value of K_{SV} than MccJ25 I13W in buffer (2.37 vs. 1.67 M^{-1}, respectively, Table 1), indicating that, although solvent exposed, the tryptophan residue becomes less accessible to the quencher when in the peptide structure, probably because of its lower diffusion coefficient respective to the tryptophan derivative NATA.

The results shown as Stern–Volmer graphs in Fig. 4 also indicated that cesium was as effective in quenching the intrinsic fluorescence emission of MccJ25 I13W when the experiment was performed in the presence or in the absence of DMPC liposomes (Fig. 4A). However, when carried out in the presence of DPPC liposomes at 27 °C, a decrease in the peptide fluorescence quenching efficiency was observed, indicating that the Trp residue of MccJ25 I13W was in a location inaccessible to the quencher when liposomes in gel phase were present in the medium (Fig. 4A). Quenching experiments with the native MccJ25 gave the same results, indicating that the change of Ile for Trp did not alter the characteristic of the peptide and its interaction with lipid bilayers (Fig. 4B).

Table 1 reports the Stern–Volmer constants calculated according to the slopes of the corresponding plots and highlights more precisely the results mentioned above.

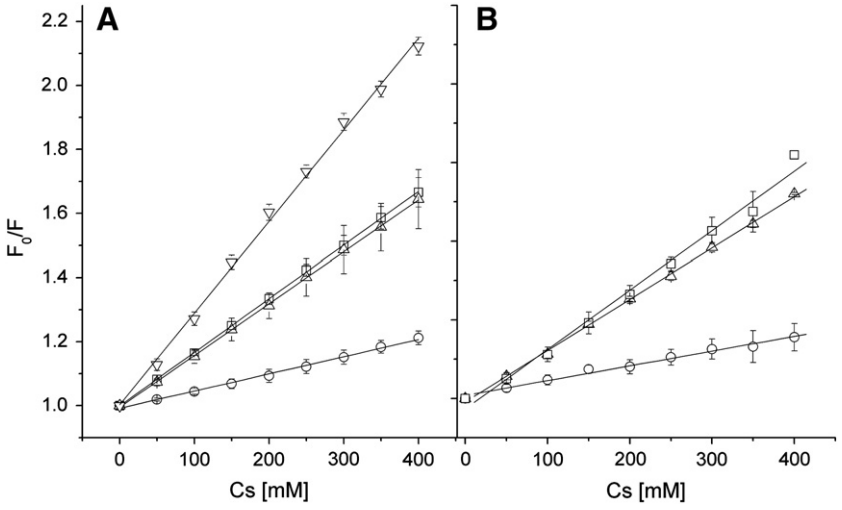

Fig. 4. Quenching of MccJ25 I13W (A) and MccJ25 (B) fluorescence emission by cesium. Samples of MccJ25I13W (2.5 μM) or MccJ25 (10 μM) dissolved in phosphate buffer pH 7.4, in the absence (□) and in the presence of DPPC (○) or DMPC (Δ) at a peptide:phospholipid molar ratio of 1:200, were incubated at 27 °C with different concentrations of CsCl. Fluorescence emission of MccJ25 and MccJ25I13W was determined at 303 or 353 nm by exciting at 277 or 288 nm, respectively. The tryptophan derivative NATA (A) was used at 3 μM final concentration and fluorescence emission at 353 nm when excited at 288 nm was recorded in the presence of increasing amounts of CsCl (▽). The results are shown as Stern–Volmer plots and represent the means ± SD of three independents experiments.

Table 1
Stern–Volmer constants of intrinsic peptide fluorescence quenching by Cs.

	K_{SV} (M^{-1})		
	MccJ25 I13W	MccJ25	*N*-acetyl-tryptophanamide
Buffer	1.67 ± 0.04	1.44 ± 0.04	2.37 ± 0.06
DPPC	0.54 ± 0.09	0.38 ± 0.09	
DMPC	1.62 ± 0.12	1.50 ± 0.12	

The Stern–Volmer constants were obtained from the slope of F_0/F at increasing concentrations of CsCl (Fig. 4). The results are the mean of three independent experiments.

Table 2
Partition coefficient and cooperative parameter of the interaction of MccJ25 I13W with liposomes.

	K_p (M^{-1})	*n*
DPPC 21 °C	5974	1.87
DPPC 12 °C	10558	2.22
DPPC:DPPS 7:3 21 °C	8385	1.79

The parameters were obtained from fitting the MccJ25 I13W intrinsic fluorescence emission increase at 335 nm upon liposome titration to the equation described in section 2.5.

3.3. Partition coefficient of MccJ25 to gel phase membranes

The increase in quantum yield of MccJ25 I13W in the presence of gel phase membranes was employed to calculate the extent of interaction with the bilayers. Partition coefficients were calculated by measuring the increase of peptide fluorescence at 335 nm, which is proportional to the amount of peptide that partitions from the aqueous phase to the lipid bilayer. As shown in Fig. 5, the MccJ25 I13W binding isotherm to DPPC liposomes in the gel phase was described by a sigmoid function, suggesting a cooperative process, with a partition coefficient K_p of 5974 M^{-1} and a cooperativity coefficient of 1.87. When the experiment was made at 12 °C instead of 21 °C, the fluorescence increase reached a plateau at lower concentrations of lipids (Fig. 5A), suggesting a higher affinity for DPPC liposomes. This was confirmed by the higher partition coefficient ($K_p = 10558\ M^{-1}$) observed in this condition (Table 2) and the increase in cooperativity coefficient.

The partition of MccJ25 I13W to DPPC liposomes was improved by increasing the negative surface charge by adding 30% of DPPS to liposomes ($K_p = 8385\ M^{-1}$, Table 2). The presence of high ionic strength in the medium did not modify the partition isotherms of MccJ25 I13W to DPPC neither DPPC:DPPS 7:3 liposomes, suggesting that predominantly the order of the lipid bilayer rather than the negative charge determines the microcin interaction with the membrane (Fig. 5B).

3.4. Studies on the insertion of MccJ25 I13W into the bilayer

In order to determine the depth of insertion of MccJ25 I13W in the lipid bilayer, intrinsic fluorescence quenching of the peptide with doxyl derivatives of stearic acid assays was performed. These fatty acid probes are modified with doxyl groups at specific positions along the hydrocarbon chain. After being added to suspensions of liposomes, these probes insert parallel to the fatty acid chains of phospholipids, positioning the doxyl group at specific depths in the hydrophobic region of the membrane and quenching the intrinsic fluorescence of the peptides. The efficiency of the fluorescence quenching is greater the closer the doxyl groups and the peptide are located.

The Stern–Volmer plots shown in Fig. 6A indicate that both 5-DS and 16-DS quenched the intrinsic fluorescence (335 nm) of the peptide when preincubated with DPPC liposomes in a peptide to phospholipd molar ratio of 1:200 at 27 °C. Also, the results showed that the 5-DS was a significantly more effective quencher than 16-DS ($K_{SV} = 11.41\ M^{-1}$ and 8.03 M^{-1} for 5-DS and 16-DS, respectively, Table 3), indicating that the Trp residue of MccJ25 I13W was located preferentially at the interfacial zone. On the other hand, no quenching was observed with either the 5-DS (Fig. 6B) or 16-DS probe (Fig. 6C) when the peptide was incubated at 27 °C in the presence of liposomes made of DMPC at 1:200 peptide to lipid molar ratio, confirming that the peptide did not insert in liquid crystal state PC bilayers.

3.5. Membrane perturbation induced by MccJ25 I13W: Permeability assays

In order to determine whether the interaction of MccJ25 I13W with DPPC liposomes produced any changes in the properties of the bilayer, we decided to perform an assay for studying the DPPC permeability to small ions. In this way, phospholipid vesicles were loaded with lithium sulfate and then suspended in isotonic buffer containing sodium sulfate. The hydrophobic cationic fluorescent probe $DiSC_3(5)$, which decreases its fluorescence emission intensity in the presence of bilayers polarized transmembrane electrochemical gradients, was used in order to evaluate differential ionic permeability.

The fluorescence emission of $DiSC_3(5)$ in the presence of loaded liposomes as a function of time is depicted in Fig. 7. It was shown that MccJ25 I13W induced membrane polarization when added to the DPPC liposomes suspension at 21 °C, this effect being proportional to the actual peptide concentration used in the experiment (Fig. 7A). In addition, a significantly lower degree of membrane polarization was

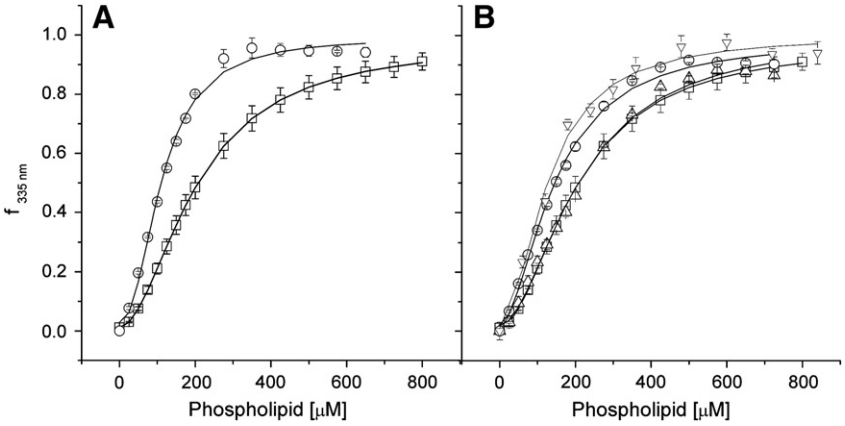

Fig. 5. Binding isotherms of peptides to DPPC liposomes. MccJ25I13W (2 μM) dissolved in phosphate buffer pH 7.4 was incubated with increasing concentrations of liposomes. The peptide fluorescence emission at 335 nm was determined by exciting at 288 nm. The parameter $I_{335\ nm}$ was calculated as described in Materials and methods. (A) Binding isotherms of MccJ25I13W to DPPC liposomes at 21 °C (□) and 12 °C (○). (B) Binding isotherms of MccJ25I13W at 21 °C to DPPC liposomes alone (□), DPPC in the presence of 1 M NaCl (Δ), a mixture of DPPC:DPPS, 7:3 (○) and DPPC:DPPS 7:3 in the presence of 1 M NaCl (▽).

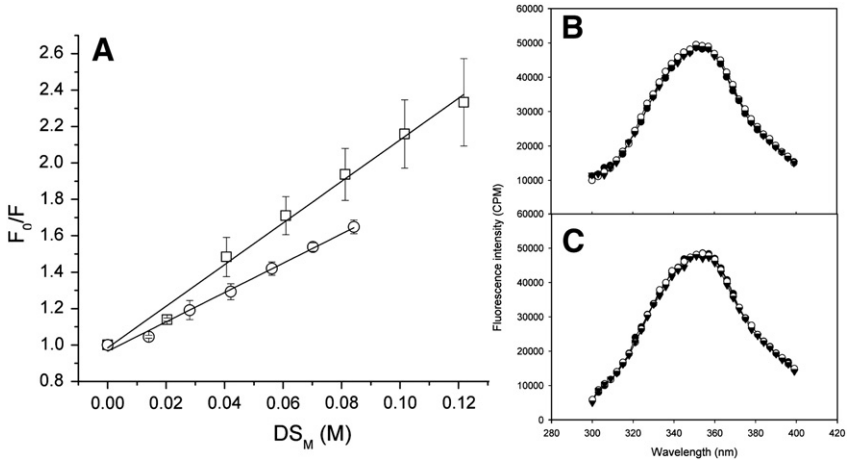

Fig. 6. Analysis of the interaction depth of MccJ25I13W with liposomes. A suspension of DPPC liposomes (0.4 mM) and MccJ25I13W (2 μM) in phosphate buffer pH 7.4 was incubated at 27 °C with increasing concentration of 5-doxyl (□) or 16-Doxyl (○) of stearic acid. Fluorescence emission of MccJ25I13W at 335 nm was determined by exciting at 288 nm. The results are the means ± SD of three experiments and shown as Stern–Volmer plots (A). The effect of 5-doxyl (B) and 16-doxyl (C) quenchers on the fluorescence emission spectra of MccJ25 I13W in the presence of DMPC liposomes at 27 °C (▼) is shown. Spectra of the peptide in buffer (○) and incubated with DMPC at 1:200 molar ratio (●) were determined by exciting at 288 nm.

observed at 55 °C with respect to that measured at 21 °C (Fig. 7B). As a positive control, 0.01% (p/v) Triton X100 was used. In this case, the increase in the $DiSC_3(5)$ fluorescence emission intensity indicated complete transmembrane potential dissipation due to the lost of membrane integrity.

4. Discussion

Biological membranes exhibit lipid and protein diffusional rates typical of bilayer fluid states. However, lateral heterogeneity is also observed as a consequence of the natural properties of lipids and proteins to segregate into domains of different composition and higher degree of order [25–27]. Thus, certain enzymes were functionally related to lipid rafts and an increasing number of peptides are being reported to interact with ordered membranes [28,29]. The effects of MccJ25 on biological membranes involve oxygen consumption cessation, deleterious oxidative species generation and respiratory chain enzymes inhibition, and were observed in bacteria and mitochondria as well [12,16,30,31]. However, in bacteria these effects seem to be a consequence of another primary target, because no revertant mutant could be naturally isolated. This primary target could be the phospholipid bilayer, the location wherein these processes take place. Interestingly, the generation of reactive oxygen species at the bacterial inner membrane can be induced by MccJ25 even though the outer membrane transporter FhuA, which carry the microcin into the bacterial cell, is inhibited [16]. This suggests that MccJ25 effects on membrane occur simultaneously with the protein mediated entrance of the peptide to cell for RNA polymerase targeting.

The mutant peptide MccJ25 I13W was shown to be a membrane-active peptide as demonstrated by fluorescence spectroscopy experiments in this work. Both the blue shift of the emission spectra and the increased quantum yield of tryptophan from MccJ25 I13W, observed only when gel phase membranes were added, strongly suggest a selective interaction of the peptide with membranes with high order degree.

Table 3
Stern–Volmer constants of intrinsic peptide fluorescence quenching by 5-doxyl and 16-doxyl stearic acid.

Quencher	K_{SV} (M^{-1})
5-DS	11.41 ± 1.73
16-DS	8.03 ± 0.82

The Stern–Volmer constants were obtained from the slope of F_0/F at increasing concentrations of doxyl-probes (Fig. 6). The results are the mean of three independent experiments.

The inhibition of the effect of water-soluble quenchers on the intrinsic fluorescence of MccJ25 I13W observed upon peptide incubation with DPPC liposomes at 27 °C confirmed that this membrane interaction was indeed a partitioning of MccJ25 I13W from the aqueous to the membrane hydrophobic phase. Experiments carried out with doxyl-labeled fatty acids showed that MccJ25 I13W penetrated into the lipid bilayer but was preferentially located near the interfacial zone of the membrane, since 5-DS was a more efficient quencher than 16-DS.

The position 13 of MccJ25 sequence lies at the extreme of the lasso structure of the peptide and was chosen for tryptophan mutation because, as previously reported, small if any perturbation in the interaction with bacterial membranes was observed for variants of MccJ25 involving this position [16,32]. Taking into account the interfacial preference of Trp^{13} in the hydrophobic lasso as indicated by the doxyl quenching experiments and that the only charge of the molecule belongs to the carboxyl group of the C-terminal Gly^{21}, which would also prefer to locate near the polar region of the membrane, the peptide would lay in a flat position along the interfacial region of the bilayer.

Liquid crystal phase membranes did not produce a blue shift of tryptophan fluorescence of MccJ25 I13W nor inhibition of fluorescence quenching by cesium. Also, the probes 5-DS and 16-DS did not quench peptide fluorescence in the presence of liquid crystal DMPC, strongly supporting the lack of interaction of MccJ25 I13W with disordered membranes.

The sigmoid dependence of the partition of MccJ25 I13W to DPPC liposomes in gel phase differs from the behavior observed with other peptides. The partition constant obtained for MccJ25 I13W was almost an order of magnitude lower compared with those reported for nystatin [20], melittin [33], cecropin [34] and equinatoxin [35]. Previous partition models were developed in response to the experimental data with polycationic peptides, which are concentrated on the surface of negatively charged membranes and which diffuse into the interface or more hydrophobic regions until repulsive electrostatic forces between peptide molecules exceed the attraction to the membrane [33], giving rise to hyperbolic partition curves. Also, changes in the peptide location at the membrane or the aggregation state as a function of the peptide/phospholipid molar ratio would give rise to deviation of the commonly observed hyperbolic partition curves [36,37]. Because the MccJ25 I13W molecule contains mostly nonpolar

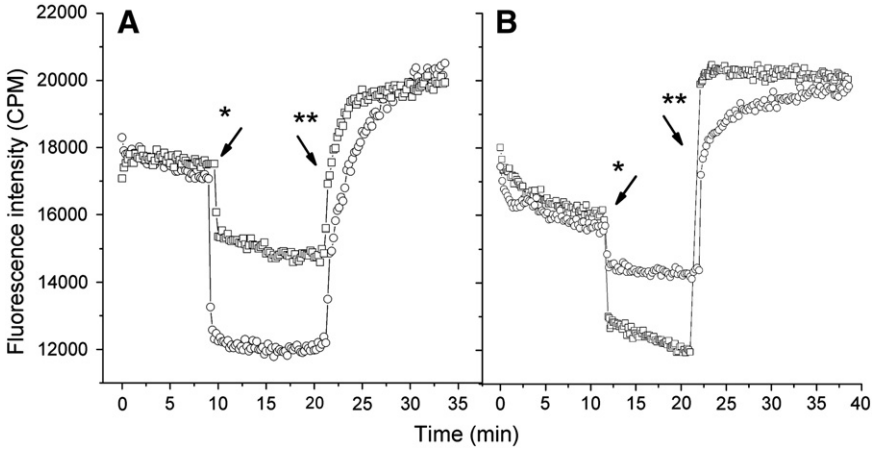

Fig. 7. Effect of MccJ25 on the permeability of DPPC liposomes. DPPC liposomes loaded with Li_2SO_4 and suspended in a buffer containing Na_2SO_4 were incubated with the fluorescent probe $DiSC_3(5)$. The timed evolution of fluorescence emission of $DiSC_3(5)$ was recorded at 677 nm by exciting at 622 nm. (A) At the indicated time (*) MccJ25 5 μM (□) or 10 μM (○) was added. (B) The effect of 10 μM MccJ25 was studied at 21 °C (□) and 55 °C (○). As a positive control of gradient dissipation, Triton X-100 was added at the specified times (**).

residues, has no net positive charge and its structure does not undergo conformational changes that promote the interaction with the bilayer, the partition of the peptide to the membrane would be driven primarily by its hydrophobic character. On the other hand, the sigmoidal behavior of the peptide partition to membrane suggests that MccJ25 I13W induces changes in the bilayer which increase its affinity to the membrane.

According to previous studies, MccJ25 would not affect significantly the membrane integrity and liposomes did not show changes in the permeability to large molecular weight substrates upon peptide membrane interaction [19]. Our results, however, showed that MccJ25 I13W induces alterations in the permeability of DPPC bilayer causing the loss of small ions. This effect, as expected, was higher in gel phase than in liquid crystalline phase vesicles. Furthermore, there was no evidence of decrease in turbidity and loss of high molecular weight molecules (not shown), suggesting no alteration of the bilayer integrity by a detergent-like action or the formation of pores, respectively.

It was postulated that packing defects of phospholipids in gel phase membrane give rise to the passage across the bilayer of ions and small polar molecules [38]. Thus, the sigmoidal behavior of the peptide partition and the increased permeability of the bilayer to small ions upon MccJ25 I13W membrane interaction suggest that the peptide would cause a disturbance in the gel phase membrane, such as packing defects that could also facilitate the entry of more peptide molecules.

Although all experiments shown in this study were performed using PC liposomes as a model of zwiterionic membrane, no effect of high ionic strength on the partition of the MccJ25 I13W to the membrane was found, indicating that mainly hydrophobic forces modulate the interaction of peptide with the bilayer. This observation is an important difference to with the case of many cationic antibiotic peptides where the electrostatic attraction with the negative phospholipids plays an almost exclusive role. Here, the presence of phospholipids with negative charges at the bilayer, although slightly increasing the peptide affinity, does not point to the surface charge of this phospholipid but toward the high T_M and high hydrocarbon chain order observed for DPPS at 27 °C as the parameters that drive the interaction of the peptide with this membrane. Although these results do not allow us to determine the mechanism of action of MccJ25 at the membrane level, we may conclude that the degree of order of the bilayer would determine the selectivity and affinity of MccJ25 I13W toward the membrane rather than the nature and charge of the phospholipids polar head. Experiments are being carried out now in our laboratory to elucidate the precise mechanism of action of MccJ25 on biological membrane.

Acknowledgements

This work was supported by Consejo Nacional de Investigaciones Científicas y Técnicas (CONICET, Argentina), Agencia de Promoción Científica y Tecnológica (FONCYT, Grants PICTO 843/04 and PAE 22642) and Secretaria de Ciencia y Técnica de la Universidad Nacional de Tucumán (CIUNT, Grant 26/D439). R.D.M. is a Career Investigator of CONICET and F.D. is a recipient of a CONICET fellowship.

References

[1] B. Bechinger, The structure, dynamics and orientation of antimicrobial peptides in membranes by multidimensional solid-state NMR spectroscopy, Biochim. Biophys. Acta 1462 (1999) 157–183.
[2] K.A. Brogden, Antimicrobial peptides: pore formers or metabolic inhibitors in bacteria? Nat. Rev. Microbiol. 3 (2005) 238–250.
[3] Y. Shai, Mode of action of membrane active antimicrobial peptides, Biopolymers 66 (2002) 236–248.
[4] Z. Oren, J.C. Lerman, G.H. Gudmundsson, B. Agerberth, Y. Shai, Structure and organization of the human antimicrobial peptide LL-37 in phospholipid membranes: relevance to the molecular basis for its non-cell-selective activity, Biochem. J. 341 (Pt 3) (1999) 501–513.
[5] L. Zhang, P. Dhillon, H. Yan, S. Farmer, R.E. Hancock, Interactions of bacterial cationic peptide antibiotics with outer and cytoplasmic membranes of *Pseudomonas aeruginosa*, Antimicrob. Agents Chemother. 44 (2000) 3317–3321.
[6] S. Duquesne, D. Destoumieux-Garzon, J. Peduzzi, S. Rebuffat, Microcins, gene-encoded antibacterial peptides from enterobacteria, Nat. Prod. Rep. 24 (2007) 708–734.
[7] K. Severinov, E. Semenova, A. Kazakov, T. Kazakov, M.S. Gelfand, Low-molecular-weight post-translationally modified microcins, Mol. Microbiol. 65 (2007) 1380–1394.
[8] P.A. Vincent, R.D. Morero, The structure and biological aspects of peptide antibiotic microcin J25, Curr. Med. Chem. 16 (2009) 538–549.
[9] K.A. Wilson, M. Kalkum, J. Ottesen, et al., Structure of microcin J25, a peptide inhibitor of bacterial RNA polymerase, is a lassoed tail, J. Am. Chem. Soc. 125 (2003) 12475–12483.
[10] K.J. Rosengren, R.J. Clark, N.L. Daly, U. Goransson, A. Jones, D.J. Craik, Microcin J25 has a threaded sidechain-to-backbone ring structure and not a head-to-tail cyclized backbone, J. Am. Chem. Soc. 125 (2003) 12464–12474.
[11] M.J. Bayro, J. Mukhopadhyay, G.V. Swapna, et al., Structure of antibacterial peptide microcin J25: a 21-residue lariat protoknot, J. Am. Chem. Soc. 125 (2003) 12382–12383.
[12] A. Bellomio, P.A. Vincent, B.F. de Arcuri, R.N. Farias, R.D. Morero, Microcin J25 has dual and independent mechanisms of action in *Escherichia coli*: RNA polymerase inhibition and increased superoxide production, J. Bacteriol. 189 (2007) 4180–4186.
[13] J. Mukhopadhyay, E. Sineva, J. Knight, R.M. Levy, R.H. Ebright, Antibacterial peptide microcin J25 inhibits transcription by binding within and obstructing the RNA polymerase secondary channel, Mol. Cell 14 (2004) 739–751.
[14] K. Adelman, J. Yuzenkova, A. La Porta, et al., Molecular mechanism of transcription inhibition by peptide antibiotic Microcin J25, Mol. Cell 14 (2004) 753–762.
[15] M.A. Delgado, M.R. Rintoul, R.N. Farias, R.A. Salomon, *Escherichia coli* RNA polymerase is the target of the cyclopeptide antibiotic microcin J25, J. Bacteriol. 183 (2001) 4543–4550.
[16] F.G. Dupuy, M.V. Chirou, B.F. de Arcuri, C.J. Minahk, R.D. Morero, Proton motive force dissipation precludes interaction of microcin J25 with RNA polymerase, but

enhances reactive oxygen species overproduction, Biochim. Biophys. Acta 1790 (2009) 1307–1313.
[17] M.R. Rintoul, B.F. de Arcuri, R.A. Salomon, R.N. Farias, R.D. Morero, The antibacterial action of microcin J25: evidence for disruption of cytoplasmic membrane energization in *Salmonella newport*, FEMS Microbiol. Lett. 204 (2001) 265–270.
[18] A. Bellomio, R.G. Oliveira, B. Maggio, R.D. Morero, Penetration and interactions of the antimicrobial peptide, microcin J25, into uncharged phospholipid monolayers, J. Colloid Interface Sci. 285 (2005) 118–124.
[19] M.R. Rintoul, B.F. de Arcuri, R.D. Morero, Effects of the antibiotic peptide microcin J25 on liposomes: role of acyl chain length and negatively charged phospholipid, Biochim. Biophys. Acta 1509 (2000) 65–72.
[20] A. Coutinho, M. Prieto, Cooperative partition model of nystatin interaction with phospholipid vesicles, Biophys. J. 84 (2003) 3061–3078.
[21] S.H. White, W.C. Wimley, A.S. Ladokhin, K. Hristova, Protein folding in membranes: determining energetics of peptide–bilayer interactions, Methods Enzymol. 295 (1998) 62–87.
[22] P.M. Matos, H.G. Franquelim, M.A. Castanho, N.C. Santos, Quantitative assessment of peptide–lipid interactions. Ubiquitous fluorescence methodologies, Biochim. Biophys. Acta 1798 (2010) 1999–2012.
[23] J.A. Poveda, M. Prieto, J.A. Encinar, J.M. Gonzalez-Ros, C.R. Mateo, Intrinsic tyrosine fluorescence as a tool to study the interaction of the shaker B "ball" peptide with anionic membranes, Biochemistry 42 (2003) 7124–7132.
[24] K. Guzow, A. Rzeska, J. Mrozek, et al., Photophysical properties of tyrosine and its simple derivatives in organic solvents studied by time-resolved fluorescence spectroscopy and global analysis, Photochem. Photobiol. 81 (2005) 697–704.
[25] S. Vanounou, D. Pines, E. Pines, A.H. Parola, I. Fishov, Coexistence of domains with distinct order and polarity in fluid bacterial membranes, Photochem. Photobiol. 76 (2002) 1–11.
[26] D.M. Engelman, Membranes are more mosaic than fluid, Nature 438 (2005) 578–580.
[27] M. Edidin, Shrinking patches and slippery rafts: scales of domains in the plasma membrane, Trends Cell Biol. 11 (2001) 492–496.
[28] M. Yoda, T. Miura, H. Takeuchi, Non-electrostatic binding and self-association of amyloid beta-peptide on the surface of tightly packed phosphatidylcholine membranes, Biochem. Biophys. Res. Commun. 376 (2008) 56–59.
[29] H.G. Franquelim, A.S. Veiga, G. Weissmuller, N.C. Santos, M.A. Castanho, Unravelling the molecular basis of the selectivity of the HIV-1 fusion inhibitor sifuvirtide towards phosphatidylcholine-rich rigid membranes, Biochim. Biophys. Acta 1798 (2010) 1234–1243.
[30] M.C. Chalon, A. Bellomio, J.O. Solbiati, R.D. Morero, R.N. Farias, P.A. Vincent, Tyrosine 9 is the key amino acid in microcin J25 superoxide overproduction, FEMS Microbiol. Lett. 300 (2009) 90–96.
[31] M.V. Niklison-Chirou, F. Dupuy, L.B. Pena, et al., Microcin J25 triggers cytochrome c release through irreversible damage of mitochondrial proteins and lipids, Int. J. Biochem. Cell Biol. 42 (2010) 273–281.
[32] A. Bellomio, P.A. Vincent, B.F. de Arcuri, R.A. Salomon, R.D. Morero, R.N. Farias, The microcin J25 beta-hairpin region is important for antibiotic uptake but not for RNA polymerase and respiration inhibition, Biochem. Biophys. Res. Commun. 325 (2004) 1454–1458.
[33] G. Beschiaschvili, J. Seelig, Melittin binding to mixed phosphatidylglycerol/phosphatidylcholine membranes, Biochemistry 29 (1990) 52–58.
[34] E. Gazit, W.J. Lee, P.T. Brey, Y. Shai, Mode of action of the antibacterial cecropin B2: a spectrofluorometric study, Biochemistry 33 (1994) 10681–10692.
[35] J.M. Caaveiro, I. Echabe, I. Gutierrez-Aguirre, J.L. Nieva, J.L. Arrondo, J.M. Gonzalez-Manas, Differential interaction of equinatoxin II with model membranes in response to lipid composition, Biophys. J. 80 (2001) 1343–1353.
[36] M.N. Melo, M.A. Castanho, Omiganan interaction with bacterial membranes and cell wall models. Assigning a biological role to saturation, Biochim. Biophys. Acta 1768 (2007) 1277–1290.
[37] F. Stauffer, M.N. Melo, F.A. Carneiro, et al., Interaction between dengue virus fusion peptide and lipid bilayers depends on peptide clustering, Mol. Membr. Biol. 25 (2008) 128–138.
[38] L.M. Loura, A. Fedorov, M. Prieto, Resonance energy transfer in a model system of membranes: application to gel and liquid crystalline phases, Biophys. J. 71 (1996) 1823–1836.